

Assessing topology and surface orientation of an antimicrobial peptide magainin 2 using mechanically aligned bilayers and electron paramagnetic resonance spectroscopy



Daniel J. Mayo, Indra D. Sahu, Gary A. Lorigan*

Department of Chemistry and Biochemistry, Miami University, Oxford, OH, 45056, United States

ARTICLE INFO

Keywords:
 Antimicrobial peptides
 Topology
 CW-EPR
 Mechanical alignment
 Glass plate alignment
 Magainin 2
 Solid phase peptide synthesis
 Electron paramagnetic resonance

ABSTRACT

Aligned CW-EPR membrane protein samples provide additional topology interactions that are absent from conventional randomly dispersed samples. These samples are aptly suited to studying antimicrobial peptides because of their dynamic peripheral topology. In this study, four consecutive substitutions of the model antimicrobial peptide magainin 2 were synthesized and labeled with the rigid TOAC spin label. The results revealed the helical tilts to be $66^\circ \pm 5^\circ$, $76^\circ \pm 5^\circ$, $70^\circ \pm 5^\circ$, and $72^\circ \pm 5^\circ$ for the TOAC substitutions H7, S8, A9, and K10 respectively. These results are consistent with previously published literature. Using the EPR (electron paramagnetic resonance) mechanical alignment technique, these substitutions were used to critically assess the topology and surface orientation of the peptide with respect to the membrane. This methodology offers a rapid and simple approach to investigate the structural topology of antimicrobial peptides.

1. Introduction

Determining the structural topology of membrane proteins with respect to the lipid bilayer is a valuable information for protein structural determination. It can provide an understanding of how membrane proteins function. Researchers using conventional biophysical tools such as NMR spectroscopy, X-ray crystallography, and electron microscopy have made many significant discoveries and continue to advance the field, but there are some shortcomings (Verardi et al., 2011; Bechinger and Burkhard, 2012; Bechinger and Salnikov, 2012; Opella and Marassi, 2004; Marassi and Opella, 2000; Yang et al., 2001). From the perspective of a structural biologist, one excellent technique that exists to assess topology comes from aligning membrane proteins inside a synthetic lipid architecture in a magnetic field (Opella and Marassi, 2004; Hong et al., 2012). Membrane alignment has been used in the past for both NMR and more recently EPR spectroscopic measurements to probe membrane orientation (Park et al., 2009; Nevzorov, 2011; Judge and Watts, 2011; Inbaraj et al., 2007; Sahu et al., 2014a).

Recently, the Lorigan lab successfully measured the distance and relative orientations between two spin labels on a membrane peripheral peptide (antimicrobial peptide magainin 2) utilizing this membrane

alignment EPR technique Sahu et al., 2014a. Membrane alignment provides a means to extract pertinent structural and dynamic information from otherwise complicated data. This information is lost using conventional methodologies. Sample alignment also simplifies the study of EPR spectra and offers a deconvolution method such that individual topological components can be analyzed. The mechanical alignment of lipid bilayers entails using a glass coverslip for support of a lipid and peptide dispersion. Planar layers of lipids form spontaneously on the glass plate surface. Mechanical alignment was developed in the Opella lab using solid-state NMR spectroscopy (Opella and Marassi, 2004; Marassi and Opella, 2000). One of the major limitations of using solid-state NMR, however, is its inherent low sensitivity. Therefore, a large amount of purification and tedious sample preparation is required to obtain high quality solid-state NMR data. Additionally, conformational heterogeneity, present in most membrane samples, can also provide another layer of complexity that must be addressed. EPR spectroscopy is advantageous to use in these experiments because it offers up to three orders of magnitude higher sensitivity than that of NMR and does not rely on expensive isotopic labels (Berliner, 2010).

EPR mechanical alignment studies rely on a rigid spin label, TOAC (2,2,6,6-tetramethyl-piperidine-1-oxyl-4-amino-4-carboxylic acid),

Abbreviations: AMPs, antimicrobial peptides; TOAC, 2,2,6,6-tetramethyl-piperidine-1-oxyl-4-amino-4-carboxylic acid; HPLC, high performance liquid chromatography; HBTU, O-Benzotriazole-N,N,N',N'-tetramethyl-uronium-hexafluoro-phosphate; TFA, trifluoroacetic acid; TIS, triisopropylsilane; CW-EPR, continuous wave electron paramagnetic resonance; NMR, nuclear magnetic resonance; DMPC, 1,2-dimyristoyl-sn-glycerol-3-phosphocholine; DHPC, 1,2-dihexanoyl-sn-glycero-3-phosphocholine; MALDI-TOF MS, matrix assisted laser desorption ionization-time of flight mass spectrometry; MOMD, macroscopic order and microscopic disorder; MLVs, multilamellar vesicles

* Corresponding author.

E-mail address: gary.lorigan@miamioh.edu (G.A. Lorigan).

which has been shown not to perturb the structure of alpha helical peptides/proteins to an appreciable extent (Nakae et al., 1983; Karim et al., 2004; Marchetto et al., 1993; Mayo et al., 2008; Marsh et al., 2007; Ghimire et al., 2009; Schreier et al., 2012; Karim et al., 2007; Vicente et al., 2015; Vicente et al., 2017; Moraes et al., 2007; Karim et al., 2006; Mangels et al., 2010). Although other rigid labels, already present in the literature could hypothetically be used, TOAC provides a direct reporter on backbone motion and superior alignment due to its limited motion (Fleissner et al., 2012; Wright et al., 2010). In this study, a model peptide magainin 2 is used to demonstrate the viability and usefulness of this technique for α -helical antimicrobial peptides (AMPs). Mechanical alignment is aptly suited for assessing antimicrobial peptides because the spectral differences between transmembrane and surface topologies are significant. Mechanical alignment data obtained by solid-state NMR spectroscopy has been reviewed in Biophysical Chemistry (Bechinger et al., 2011).

Antimicrobial peptides are present in many organisms ranging from plants to humans and are significant players in the animal kingdom (Bevins and Salzman, 2011; Ausubel, 2005). AMPs serve as an innate immune response against a broad spectrum of microbial species, and AMPs are capable of warding off and thwarting bacteria, fungi and viruses (Nguyen et al., 2011). They are of particular interest recently because of their potential application to limit the growth of antibiotic resistant bacteria (Sato and Felix, 2006). One class of AMPs that has been extensively investigated are alpha helical AMPs. These peptides are generally longer than the thickness of the bilayer and predominantly lie on the surface of the membrane at low concentrations. Magainin 2 is one such peptide and serves as an excellent model peptide because it was one of the first AMP identified and isolated from the skin of the African clawed frog (Zasloff and Magainins, 1987). It has several interesting functional aspects including a thinning effect of the membrane that is thought to exert positive strain curvature on the membrane surface and induce toroidal pores (Bechinger and Burkhard, 2012; Matsuzaki et al., 1994; Matsuzaki et al., 1998a; Matsuzaki et al., 1998b; Karal et al., 2015). However, the transient “toroidal pore” model is very challenging to directly study and has been shown to depend on various experimental conditions, such as the identity of the lipids in the study, lipid concentration, peptide concentration, and the introduction of other physiological biomolecules. Therefore, the pore formation mechanism continues to remain unclear (Tamba and Yamazaki, 2009; Bechinger, 2015). In this study, we synthesized four consecutive substitutions of the antimicrobial peptide magainin 2 and labeled with the rigid TOAC spin label to probe the topology and surface orientation of the peptide with respect to the membrane.

2. Experimental section

2.1. Materials

Chemicals and amino acids needed for peptide synthesis were purchased from Applied Biosystems Inc. (Foster City, CA). Wang resin was obtained from Novabiochem, 1,2-dimyristoyl-sn-glycerol-3-phosphocholine (DMPC) was purchased from Avanti Polar Lipids Inc., and 2,2,2-trifluoroethanol (TFE) was acquired from Sigma Aldrich. Glass cover slips were bought from Marienfeld laboratory glassware (Lauda-Königshofen, Germany). Deuterium-depleted water was purchased from Isotec Inc. (Miamisburg, OH). Double-distilled water can alternately be used to prepare these solutions.

2.2. Peptide synthesis of magainin 2

The procedure for synthesizing magainin 2 has been well-established (Mayo et al., 2008; Matsuzaki et al., 1994). A 433A Peptide Synthesizer, Applied Biosystems Inc., (Foster City, CA) was used for the studies. A UV detector was attached to this system to assess the coupling efficiency for each amino acid in the peptide. Peptides were

synthesized using Fmoc chemistry, and a 0.1 mmol protocol was provided in the SynthAssist 2.0 software from Applied Biosystems. The coupling agent used was O-benzotriazole-N,N,N',N'-tetramethyl-uronium-hexafluoro-phosphate (HBTU). A high substitution resin (0.71 mmol/g) was used. The wild-type magainin 2 sequence is shown below along with the TOAC-labeled peptides synthesized for this study:

WT: $\text{NH}_2\text{C}^{11}\text{I}^2\text{G}^3\text{K}^4\text{F}^5\text{L}^6\text{H}^7\text{S}^8\text{A}^9\text{K}^{10}\text{K}^{11}\text{F}^{12}\text{G}^{13}\text{K}^{14}\text{A}^{15}\text{F}^{16}\text{V}^{17}\text{G}^{18}\text{E}^{19}\text{I}^{20}\text{M}^{21}\text{N}^{22}\text{S}^{23}\text{-COOH}$

H7: $\text{NH}_2\text{G}^{11}\text{I}^2\text{G}^3\text{K}^4\text{F}^5\text{L}^6\text{H}^7\text{TOAC}^7\text{S}^8\text{A}^9\text{K}^{10}\text{K}^{11}\text{F}^{12}\text{G}^{13}\text{K}^{14}\text{A}^{15}\text{F}^{16}\text{V}^{17}\text{G}^{18}\text{E}^{19}\text{I}^{20}\text{M}^{21}\text{N}^{22}\text{S}^{23}\text{-COOH}$

S8: $\text{NH}_2\text{G}^{11}\text{I}^2\text{G}^3\text{K}^4\text{F}^5\text{L}^6\text{H}^7\text{TOAC}^8\text{A}^9\text{K}^{10}\text{K}^{11}\text{F}^{12}\text{G}^{13}\text{K}^{14}\text{A}^{15}\text{F}^{16}\text{V}^{17}\text{G}^{18}\text{E}^{19}\text{I}^{20}\text{M}^{21}\text{N}^{22}\text{S}^{23}\text{-COOH}$

A9: $\text{NH}_2\text{G}^{11}\text{I}^2\text{G}^3\text{K}^4\text{F}^5\text{L}^6\text{H}^7\text{S}^8\text{TOAC}^9\text{K}^{10}\text{K}^{11}\text{F}^{12}\text{G}^{13}\text{K}^{14}\text{A}^{15}\text{F}^{16}\text{V}^{17}\text{G}^{18}\text{E}^{19}\text{I}^{20}\text{M}^{21}\text{N}^{22}\text{S}^{23}\text{-COOH}$

K10: $\text{NH}_2\text{G}^{11}\text{I}^2\text{G}^3\text{K}^4\text{F}^5\text{L}^6\text{H}^7\text{S}^8\text{A}^9\text{TOAC}^{10}\text{K}^{11}\text{F}^{12}\text{G}^{13}\text{K}^{14}\text{A}^{15}\text{F}^{16}\text{V}^{17}\text{G}^{18}\text{E}^{19}\text{I}^{20}\text{M}^{21}\text{N}^{22}\text{S}^{23}\text{-COOH}$

2.3. Peptide purification

Peptides were cleaved with a mixture consisting of 85% trifluoroacetic acid (TFA), 5% H_2O , 5% anisole, and 5% triisopropylsilane (TIS). Peptides were then purified by reverse-phase HPLC (high performance liquid chromatography). A C4 preparative HPLC column was used to purify all peptide substitutions. A two-solvent system was used consisting of water + 0.1% TFA and 90% acetonitrile + 10% water + 0.1% TFA. The purity was then assessed by analytical HPLC. The purity of all peptides was > 95%. Purified peptides were lyophilized and stored at -20°C . After lyophilization the peptides were dissolved in 10% ammonium hydroxide and left at room temperature for 3–4 h. The peptide solution was then lyophilized to obtain the peptide.

All synthesized and purified peptides were analyzed by a Bruker AutoFlexIII MALDI-TOF MS to verify the mass of all peptides.

2.4. Sample preparation

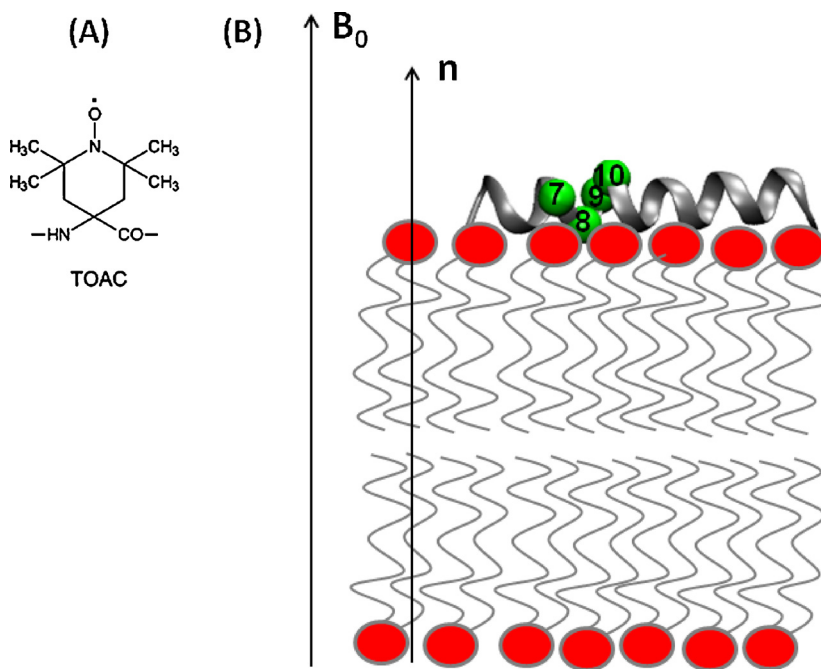
Lipid-peptide samples were prepared in a 1.5 mL centrifuge tubes by adding 50 μL of TFE and 50 μL of chloroform to $\sim 50\ \mu\text{g}$ of previously lyophilized peptide. DMPC (6 mg) in 300 μL of chloroform was then added to the centrifuge tube. The solution was then reduced to 100 μL and delivered onto five glass coverslips (6 \times 10 mm). The thickness of the glass coverslip was 0.06–0.08 mm. The final peptide to lipid ratio was 1: \sim 250. The glass plates were allowed to dry for 30 min and vacuum desiccated overnight (12 h). Samples were then hydrated by adding 4 μL of water and placed in a hydration chamber with a relative humidity of 93% for 12 h at 42°C .

2.5. EPR spectroscopy

Each sample was mounted on a quartz rod using double sided tape and inserted into the EPR cavity. Samples were perpendicular- and parallel-oriented with respect to the magnetic field by twisting the quartz rod. All experiments were performed on a Bruker EMX X-band CW-EPR spectrometer using the following experimental parameters: 100 G sweep width, 42 s sweep time, 9.434 GHz microwave frequency, 100 kHz modulation frequency, 1.0 G modulation amplitude, microwave power of 10 mW, and a temperature of 45°C .

2.6. EPR spectral simulations

Each EPR spectrum was analyzed using the nonlinear least-squares (NLSL) analysis program developed by Freed and co-workers (Schneider and Freed, 1989; Budil et al., 1996). All randomly-dispersed EPR spectra were analyzed using the MOMD (macroscopic order and microscopic disorder) model incorporated into the NLSL program. Aligned data were simulated using NLSL simulations with the introduction of the director tilt angle (ψ) in the similar way reported in



the literature (Ghimire et al., 2012a). The order parameters were determined by varying the ordering potential coefficients c_{20} , c_{22} during the simulations in the same way reported in the literature (Mayo et al., 2008). During simulations, A , g , linewidths, and the dynamic parameters were refined using the starting set of hyperfine and g -tensor parameters from previous studies (Mayo et al., 2008). Each randomly-dispersed sample was simulated with 40 different orientations to get full convergence (Ghimire et al., 2012a, 2012b).

2.7. EPR calculations

The director tilt and helical tilt angles were calculated based on the method previously described in our lab (Inbaraj et al., 2007; Inbaraj et al., 2006; Karp et al., 2006). The coordinate axes for the nitroxide spin label have been defined previously in the literature (Inbaraj et al., 2007; Karp et al., 2006). Briefly, the x-axis extends along the N–O bond, the z-axis along the p-orbital of the nitrogen, and the y-axis is orthogonal to the x- and z-axes. With the axes defined, the hyperfine tensor components are also defined. In this rigid label system, the electron density is axially symmetric along the x- and y-axis such that their hyperfine tensor values are $A_{xx} \approx A_{yy} \ll A_{zz}$. Using this fact the following equations can be written:

$$A_{\perp} = \frac{1}{2}(1 - \langle \cos^2 \theta \rangle)(A_{zz} - A_{xx}) + A_{xx} \quad (1)$$

$$A_{\parallel} = \langle \cos^2 \theta \rangle(A_{zz} - A_{xx}) + A_{xx} \quad (2)$$

where θ is defined as the angle between the z-axis of the nitroxide label and the axis of motional averaging (Z_D).

When the system has no motion, θ is negligible and A_{zz} (A_{\parallel}) is experimentally observed, if the magnetic field is applied along the z-axis. In aligned samples, if the magnetic field is applied along the Z_D axis, the hyperfine coupling A_{\parallel} is observed. However, if the magnetic field is applied perpendicular to Z_D , A_{\perp} can be measured. The generalized Eq. (3) can be written when the magnetic field makes an arbitrary angle ψ with the axis of motional averaging (Z_D). Using Eq. (3) and Eq. (4) the director tilt and helical tilt can be calculated using the experimental parameters defined previously (Inbaraj et al., 2007; Inbaraj et al., 2006).

Fig. 1. (A) Chemical structure of the TOAC spin label probe, (B) Schematic representation of the magainin 2 peptide with the TOAC spin labeling sites represented by green spheres at their alpha carbons in a peripheral orientation with respect to the phospholipid bilayers. n represents the phospholipid bilayer normal, and B_0 represents the applied static magnetic field. (For interpretation of the references to colour in this figure legend, the reader is referred to the web version of this article.)

$$A_{\text{exp}} = (A_{\parallel}^2 \cos^2 \psi + A_{\perp}^2 \sin^2 \psi)^{\frac{1}{2}} \quad (3)$$

$$\cos \psi = \sin(\beta_n) \cdot \cos(\alpha_n) \cdot \sin(\beta_D) \cdot \cos(\alpha_D) + \sin(\beta_n) \cdot \sin(\alpha_n) \cdot \sin(\beta_D) \cdot \sin(\alpha_D) + \cos(\beta_n) \cdot \cos(\beta_D) \quad (4)$$

where, (α_n, β_n) and (α_D, β_D) are reduced Eulers' angle of rotation in two frame of references (n , Z_D) respectively.

3. Results

Previously, we probed the topology of the antimicrobial peptide magainin 2 oriented on the surface of magnetically aligned phospholipid bilayers (bicelles) using spin labeled EPR spectroscopy as a proof of concept (Mayo et al., 2008). Our previous continuous wave (CW) EPR dipolar broadening study indicated no significant secondary structural perturbation due to incorporation of TOAC on magainin 2 (Sahu et al., 2014a). In this study, we investigated the topology and surface orientation of the magainin 2 peptide in a more detail by analyzing mechanically aligned EPR data from four consecutive individual TOAC labeled magainin 2 constructs: H7, S8, A9, and K10. Fig. 1 shows sites and probes, and the alignment scheme for magainin 2 in lipid bilayers.

3.1. CW-EPR spectra of aligned and randomly dispersed samples

Fig. 2 shows CW-EPR spectra of four TOAC-labeled magainin 2 samples. The randomly-dispersed (top panel) and parallel-aligned (bottom panel) EPR data were collected at 318 K. In the case of the randomly-dispersed EPR data, DMPC multilaminar vesicles (MLVs) were used. The experimental spectra are shown in black, while the red spectra are the best-fitted NLSL simulations of the data. The randomly dispersed magainin 2 CW-EPR spectra, shown in the top panel of Fig. 2: (A) H7, (B) S8, (C) A9, (D) K10, have a similar line shape and are devoid of topological information. The orientation of the spin label with respect to the magnetic field in these spectra is randomly-distributed. A minor sharp isotropic component is also observed in several of the EPR spectra. The component arises from another population of magainin 2 or free label present and varies slightly in intensity between the substitutions. These features are also less noticeable at 298 K (data not shown). This phenomenon has been documented in the past for aligned

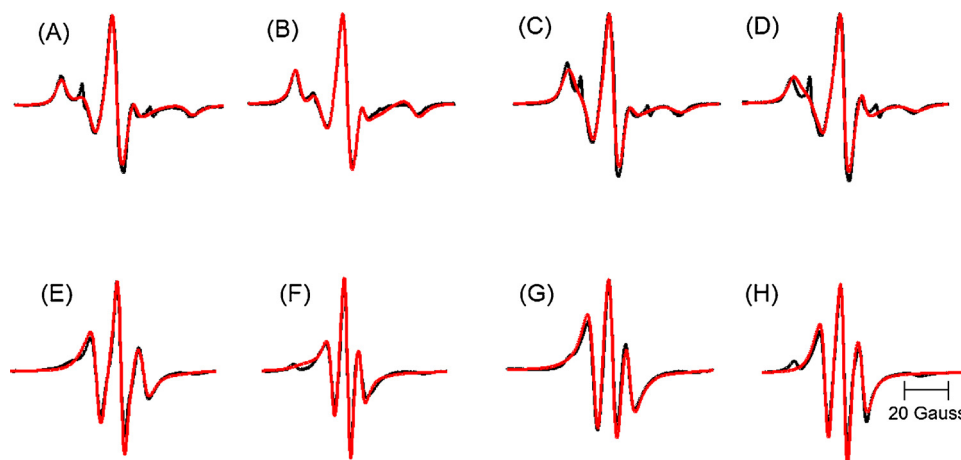


Fig. 2. X-Band CW-EPR spectra of magainin 2 incorporated into randomly dispersed DMPC bilayers of (A) TOAC7, (B) TOAC8, (C) TOAC9, and (D) TOAC10 and incorporated into parallel, mechanically-aligned DMPC lipid bilayers (E) TOAC7, (F) TOAC8, (G) TOAC9, (H) TOAC10. The black lines are experimental EPR data, and the red lines are the corresponding best-fit NLSL simulations. (For interpretation of the references to colour in this figure legend, the reader is referred to the web version of this article.)

and randomly-oriented samples and does not affect the hyperfine splitting values obtained from the spectra and thus does not influence the conclusions drawn from the results (Ghimire et al., 2012b; Dzikovski et al., 2004).

The CW-EPR spectra of the four parallel-aligned, singly-labeled TOAC labeled magainin 2 samples are shown in Fig. 2: (E) H7, (F) S8, (G) A9, (H) K10. The inspection of EPR spectra in Fig. 2 clearly indicates that there are substantial spectral differences in the data for aligned samples when compared to the data for randomly dispersed samples. The significant decrease in hyperfine splitting observed in the aligned spectra is due to the high degree of spectral anisotropy that exists in the labeled peptides.

Additionally, a small unoriented component is also observed in some of the aligned spectra. Most likely this is either due to spin label hysteresis or lipid deformation at the end of the glass plate (Ghimire et al., 2012b; Karp et al., 2006). This small unoriented component was also observed in the parallel aligned samples when varying concentrations of spin labeled lipid 5-DSA was added (data not shown).

3.2. Director and helical tilt

Earlier studies have established a methodology using EPR experimental observables to extract the helical tilt angle (Φ) between the helical axis (h) and the bilayer normal (n) for the purpose of determining the degree a helical protein is tilted with respect to the membrane (Mayo et al., 2008). Using the same matrix algebra, the angle Φ can be obtained from the angle ψ , which is the angle between the director tilt vector (Z_D) and the bilayer normal (n). Here, Z_D can be thought of as the axis of average spin label motion. To determine this angle, A_{exp} from the parallel-aligned EPR spectra, and A_{\parallel} and A_{\perp} from the randomly distributed samples were measured and are provided in Table 1.

The director tilt or the average axis of the spin label motion, which exists about the TOAC spin label, was then calculated using Eq. (3), shown in Table 1. The results for the TOAC substitutions H7, S8, A9, and K10 are $71^\circ \pm 5^\circ$, $80^\circ \pm 5^\circ$, $75^\circ \pm 5^\circ$, and $77^\circ \pm 5^\circ$, respectively and vary roughly by 9° . The TOAC-label axis of the director tilt in alpha helical peptides, makes an angle of 21° with respect to the helical axis (Inbaraj et al., 2006; FlippinAnderson et al., 1996; Hanson et al., 1998). Using this angle, the helical tilt can be calculated using the Euler rotational matrices of three Euler angles (α , β , γ) by solving Eq. (4). The helical tilt for the TOAC substitutions H7, S8, A9, and K10 are $66^\circ \pm 5^\circ$, $76^\circ \pm 5^\circ$, $70^\circ \pm 5^\circ$, and $72^\circ \pm 5^\circ$, respectively, and again vary roughly by 9° . These values can also be found in Table 1.

Table 1

Measured hyperfine values obtained from experimental data in the parallel, and randomly dispersed samples. The director tilt values were obtained from the parallel aligned samples and the helical tilt values were obtained from the director tilt. The uncertainties in these angles are $\pm 5^\circ$.

Sites	Parallel (A_{exp}) (G)	Randomly Dispersed (A_{\parallel} , A_{\perp}) (A_{min} , A_{max}) (G)	Experimental Director Tilt ($^\circ$)	Experimental Helical Tilt ($^\circ$)
H7	11.9	(6.8, 30.8)	71	66
S8	7.9	(6.1, 29)	80	76
A9	9.3	(6.2, 27)	75	70
K10	9.5	(6.7, 29.7)	77	72

3.3. Spectral simulations

The CW-EPR spectra were simulated based on MOMP or Brownian motion diffusion theory using the NLSL approach developed by Freed et al. (Schneider and Freed, 1989; Budil et al., 1996) MOMP simulation parameters are shown in Table 2. The variance in the values obtained from the NLSL simulations and the experimental results are small because of the superior fit obtained for the spectra. The order parameter and rotational correlation times are consistent with previous reports in the literature (Mayo et al., 2008). Table 2 shows that the rotational correlation time (τ_c) varies between 12 and 19 ns for parallel aligned samples when compared to 10–13 ns for randomly dispersed samples. These data suggest that the local dynamics of TOAC labeled sites are more resolved in aligned samples when compared to the randomly dispersed samples. This is consistent with the previously published EPR alignment studies (Sahu et al., 2017). Table 2 shows that the order

Table 2

EPR parameters obtained from NLSL simulations in the parallel and randomly-dispersed samples. The uncertainties in these angles are $\pm 5^\circ$.

Sites		Correlation time (τ_c , ns)	S_{20}	S_{22}	Director Tilt ($^\circ$) (simulation)	Helical Tilt ($^\circ$) (simulation)
H7	aligned	12	0.7	0.2	71	67
	random	10	0.4	0.3		
S8	aligned	19	0.7	0.1	82	78
	random	13	0.4	0.3		
A9	aligned	14	0.6	0.1	75	71
	random	10	0.3	0.1		
K10	aligned	15	0.6	0.2	77	72
	random	13	0.4	0.3		

parameters obtained from NLSL simulation results vary between S_{20} of 0.6–0.7 and S_{22} of 0.1–0.2 for parallel aligned samples when compared to S_{20} of 0.3–0.4 and S_{22} of 0.1–0.3 for randomly dispersed samples. Similarly, the director tilt angles obtained from NLSL simulation results for the TOAC substitutions H7, S8, A9, and K10 are $71^\circ \pm 5^\circ$, $82^\circ \pm 5^\circ$, $75^\circ \pm 5^\circ$, and $77^\circ \pm 5^\circ$, respectively and vary roughly by 12° . The corresponding helical tilt for the TOAC substitutions H7, S8, A9, and K10 are $67^\circ \pm 5^\circ$, $78^\circ \pm 5^\circ$, $71^\circ \pm 5^\circ$, and $72^\circ \pm 5^\circ$, respectively, and again vary roughly by 11° . The NLSL simulation results are in well agreement with the experimental results (Table 1).

4. Discussion

In previous studies, CW-EPR spectrum of parallel-aligned surface peptides have shown a significant reduction in the hyperfine splitting due to the orientation of A_{xx} and A_{yy} with respect to B_0 (Mayo et al., 2008). Consequently from the EPR spectra of parallel aligned samples obtained for this study, the A_{exp} values are greatly reduced when compared to those of the EPR spectra of randomly-dispersed samples. Typical values for the nitroxide hyperfine tensor are $A_{xx} = 6$ G, $A_{yy} = 6$ G, and $A_{zz} = 33$ G. In parallel-aligned spectra, the x- and y-tensor components are motionally averaged, and the hyperfine coupling observed therefore is dramatically reduced. The perpendicular spectra were omitted because a powder contribution was observed in the alignment due to the random orientation of A_{xx} , A_{yy} , A_{zz} of magainin 2 on the surface of the membrane (Fig. 3).

From the helical tilt angle calculation it is obvious that all substitutions of magainin 2 lie on the surface of the membrane with a preferred average tilt of $71 \pm 5^\circ$. The NLSL-simulated spectra also provide an average tilt of $72 \pm 5^\circ$. Previously we reported a helical tilt angle of $81 \pm 4^\circ$ for the TOAC labeled site S8 (Mayo et al., 2008). In the present work, the same S8 site was also reproduced with the value of $76 \pm 5^\circ$ which is consistent with the previous result within the experimental uncertainty. Ulmschneider et al. has reported a helical tilt angle of $87 \pm 7^\circ$ for magainin using a computational approach (Ulmschneider et al., 2006). The results are also close to several solid-state NMR results of a topology of ~ 80 – 90° with respect to the membrane normal (Mayo et al., 2008; Strandberg et al., 2009; Marassi et al., 2000; Strandberg et al., 2016). Interestingly, the helical tilt values obtained exhibit a variance between the TOAC labels placed at the different amino acids, more specifically, the H7 substitution has lower value of 66° . The relatively lower tilt angle obtained for H7 may be due

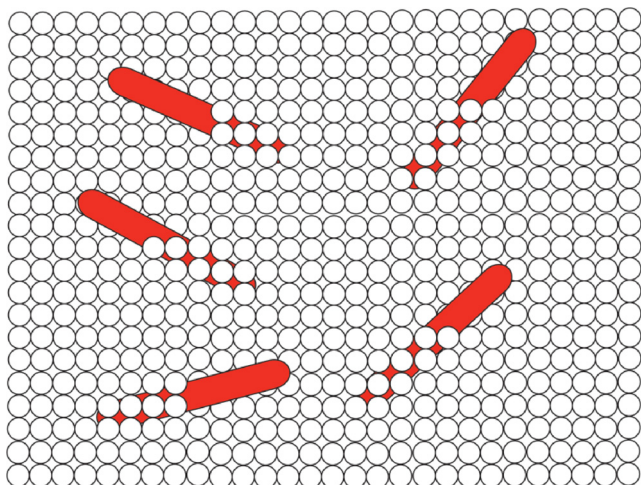


Fig. 3. Depiction of magainin 2 randomly oriented on the surface of the lipid membrane.

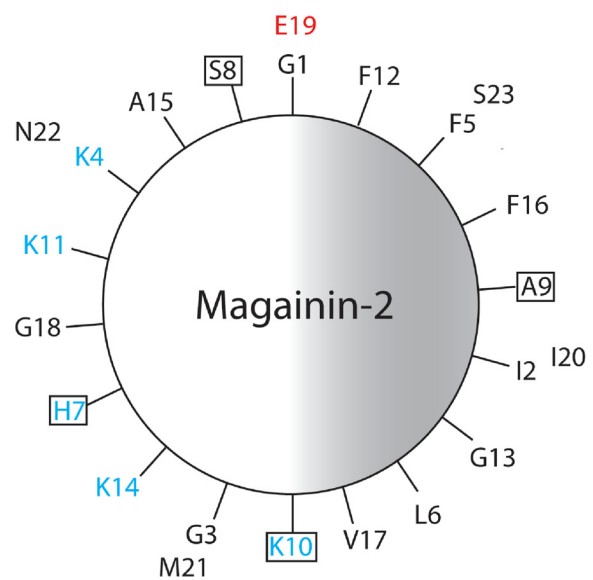


Fig. 4. Helical wheel representation of Magainin 2. Positive and negative charged residues are illustrated as blue and red respectively. The TOAC-substituted positions are represented by boxed amino acids (Strandberg et al., 2009). (For interpretation of the references to colour in this figure legend, the reader is referred to the web version of this article.)

fact that the TOAC nitroxide moiety is solvent exposed. The helical tilt for the residues closest to the membrane surface corresponding, seems to change very little. Magainin 2 has been shown to lie specifically with its positively-charged amino acids facing away from the membrane surface (Strandberg et al., 2009; Marassi et al., 2000). From the helical wheel shown in Fig. 4, it is clear that TOAC at A9 is buried in the membrane, while the H7 substitution is facing away from the membrane. Previous studies in the literature have shown that an increase in hyperfine splitting is observed for water exposed spin labels such as TOAC (Marsh, 2010; Steinhoff et al., 2000; Plato et al., 2002). The deviation in helical tilt therefore is due to the accessibility to the polar environment. This phenomenon explains why the H7 and A8 substitutions have a slightly lower and higher helical tilt. Again, these unique results were only feasible using alignment methodologies. Aisenbrey and Bechinger (2004) has also observed powder pattern line shapes for solid-state NMR samples at the helical tilt close to 90° (Aisenbrey and Bechinger, 2004). Gesell et al. (1997) reported that the three dimensional structure of magainin 2 is helical having a curvature or kink around residues 12 and 13 (Gesell et al., 1997). The curvature is concave towards the hydrophobic face of the peptide (Gesell et al., 1997). The variation in the helical tilt angle corresponding to different sites of the peptide revealed in this study is also consistent with the curved/kinked nature of magainin 2. This is complementary information about the helical tilt of magainin 2 obtained using the mechanically aligned EPR technique when compared to solid-state NMR spectroscopic methods. In this study, we have used DMPC lipids for the formation of lipid bilayers, whereas NMR studies have used different lipids or a combination of lipids. The deviation of the helical tilt from NMR results might be due to the variation in the types of lipids used in the study, curvature of the peptide, and the error introduced in the proper sample alignment.

Mechanical alignment has significant implications for determining pertinent biological mechanisms of peptides. If pores were to be observed, a significantly lower hyperfine value would be exhibited for the parallel-aligned samples. With the concentrations of magainin 2 used in these experiments, pores were not observed with DMPC lipids, which is

comparable with the previously published solid-state NMR studies (Strandberg et al., 2009). However, the methodology presented here is a viable path to pursue in the future using other negatively-charged lipids mimicking the bacterial membrane surface. Previous studies have shown that negatively-charged membranes significantly increase the potency of magainin 2 (Matsuzaki et al., 1997; Tamba and Yamazaki, 2005).

Under the conditions used in these experiments, magainin 2 is observed to lie parallel with respect to the lipid bilayer at all positions. These results suggest that under the experimental conditions used, magainin 2 does not produce pores that lie parallel with the bilayer normal. This observation is inconsistent with the barrel-stave model where a population would always be oriented parallel to the membrane normal (Yamaguchi et al., 2001). As observed from the parallel orientation, the peptide remains in the plane of the membrane. Other peptide mechanisms have also been deduced in a similar fashion using solid-state NMR spectroscopy (Yamaguchi et al., 2001). Future study of molecular dynamics simulation can provide additional insight on how magainin 2 interact with lipid bilayers.

Solid-state NMR spectroscopy has been used to confirm a helical structure in oriented bilayers from four consecutive labels (Bechinger et al., 1993). The combined use of ¹⁵N and ²H labeling can provide better solid-state NMR structural restraints (Michalek et al., 2013). A periodic data profile can be obtained when the inverse linewidth mobility is scanned against the amino acid sequence of the protein using EPR spectroscopy. This periodic data profile reflects the local secondary structure of the protein (Cuello et al., 2004; Klug and Feix, 2008; Sahu et al., 2013). EPR data obtained on the oriented samples can also be used as additional restraints to refine the protein structure (Sahu et al., 2014b).

Determining the structural topology of antimicrobial peptides can be a difficult task even with sophisticated technologies like neutron scattering, oriented circular dichroism (OCD), fluorescence, FT-IR, and solid-state NMR biophysical techniques (Marassi et al., 2000; Bechinger et al., 1993; Prongidi-Fix et al., 2007; Matsuzaki et al., 1996; Huang, 2000; Oren and Shai, 1998; Bechinger et al., 1992; Jackson et al., 1992). Solid-state NMR spectroscopic techniques provide perhaps the most comprehensive information of peptides in the native environment, ranging from topology, dynamics, atomic resolution, and their underlying mechanisms. Given the number of variables that can be changed between experiments, EPR glass plate alignment provides an excellent method to assess the topology with a small amount of sample (order of microgram) and a shorter data acquisition time (order of minutes). Although the EPR mechanical alignment technique provides complementary information about the protein topology, the incorporation of a rigid spin label such as TOAC on the larger membrane protein via bacterial overexpression is challenging. Future studies will be required to check the functional activities of the TOAC labeled magainin 2 peptide to enhance the implication of these results. A simultaneous analysis of all four data sets will be useful for obtaining a more reliable helical tilt value.

5. Conclusion

CW-EPR glass plate alignment has been shown in this study to be a compelling method to determine the topology of antimicrobial peptides and can be done in an amino acid sequence dependent manner. The quantitative helical tilt angles determined in this study are close to the previous magainin 2 studies (Mayo et al., 2008). From this study, EPR mechanical alignment is shown to be an excellent method to study how antimicrobial peptides are oriented with respect to the phospholipid bilayer. It also has a significant value for assessing topological changes of other antimicrobial peptides and their underlying mechanisms. Mechanical alignment may also be a strong method to study multi-component peptide systems and determine potential conformational changes and their orientational changes with respect to the membrane.

Funding sources

NIGMS/NIH Maximizing Investigator's Research Award (MIRA) R35 GM126935. National Science Foundation Grant CHE-1807131. National Institutes of Health Grant R01 GM108026. National Science Foundation Grant CHE-1305664.

Conflict of interest statement

The authors declare no competing financial interest.

Acknowledgments

This work was generously supported by the National Science Foundation Grants CHE-1305664, CHE-1807131 and NIGMS/NIH Maximizing Investigator's Research Award (MIRA) R35 GM126935 award and a NIHGM R01 GM108026. Gary A. Lorigan would also like to acknowledge support from the John W. Steube Professorship.

References

- Aisenbrey, C., Bechinger, B., 2004. Investigations of polypeptide rotational diffusion in aligned membranes by H-2 and N-15 solid-state NMR spectroscopy. *J. Am. Chem. Soc.* 126 (50), 16676–16683.
- Ausubel, F.M., 2005. Are innate immune signaling pathways in plants and animals conserved? *Nat. Immunol.* 6 (10), 973–979.
- Bechinger, E.S.S., Burkhardt, 2012. Lipid-Controlled peptide topology and interactions in bilayers: structural insights into the synergistic enhancement of the antimicrobial activities of PGLa and magainin 2. *Biophys. J.* 100 (6), 1473–1480.
- Bechinger, B., Salnikov, E.S., 2012. The membrane interactions of antimicrobial peptides revealed by solid-state NMR spectroscopy. *Chem. Phys. Lipids* 165 (3), 282–301.
- Bechinger, B., Zasloff, M., Opella, S.J., 1992. Structure and interactions of magainin antibiotic peptides in lipid bilayers: a solid-state nuclear magnetic resonance investigation. *Biophys. J.* 62 (1), 12–14.
- Bechinger, B., Zasloff, M., Opella, S.J., 1993. Structure and orientation of the antibiotic peptide magainin in membranes by solid-state nuclear magnetic resonance spectroscopy. *Protein Sci.* 2 (12), 2077–2084.
- Bechinger, B., Resende, J.M., Aisenbrey, C., 2011. The structural and topological analysis of membrane-associated polypeptides by oriented solid-state NMR spectroscopy: established concepts and novel developments. *Biophys. Chem.* 153 (2–3), 115–125.
- Bechinger, B., 2015. The SMART model: Soft Membranes Adapt and Respond, also Transiently, in the presence of antimicrobial peptides. *J. Pept. Sci.* 21 (5), 346–355.
- Berliner, L.J., 2010. From spin-labeled proteins to *in vivo* EPR applications. *Eur. Biophys. J.* 39 (4), 579–588.
- Bevins, C.L., Salzman, N.H., 2011. Paneth cells, antimicrobial peptides and maintenance of intestinal homeostasis. *Nat. Rev. Microbiol.* 9 (5), 356–368.
- Budil, D.E., Lee, S., Saxena, S., Freed, J.H., 1996. Nonlinear-Least-Squares analysis of slow-motion EPR spectra in one and two dimensions using a modified Levenberg–Marquardt algorithm. *J. Magn. Reson. Ser. A* 120, 155–189.
- Cuello, L.G., Cortes, D.M., Perozo, E., 2004. Molecular architecture of the KvAP voltage-dependent K⁺ channel in a lipid bilayer. *Science* 306 (5695), 491–495.
- Dzikovski, B.G., Borbat, P.P., Freed, J.H., 2004. Spin-labeled gramicidin a: channel formation and dissociation. *Biophys. J.* 87 (5), 3504–3517.
- Fleissner, M.R., Bridges, M.D., Brooks, E.K., Cascio, D., Kálai, T., Hideg, K., Hubbell, W.L., 2012. Structure and dynamics of a conformationally constrained nitroxide side chain and applications in EPR spectroscopy. *Proc. Natl. Acad. Sci. U. S. A.* 108 (39), 16241–16246.
- FlippenAnderson, J.L., George, C., Valle, G., Valente, E., Bianco, A., Formaggio, F., Crisma, M., Toniolo, C., 1996. Crystallographic characterization of geometry and conformation of TOAC, a nitroxide spin-labelled C-alpha,C-alpha-disubstituted glycine, in simple derivatives and model peptides. *Int. J. Pept. Protein Res.* 47 (4), 231–238.
- Gesell, J., Zasloff, M., Opella, S.J., 1997. Two-dimensional H-1 NMR experiments show that the 23-residue magainin antibiotic peptide is an alpha-helix in dodecylphosphocholine micelles, sodium dodecylsulfate micelles, and trifluoroethanol/water solution. *J. Biomol. NMR* 9 (2), 127–135.
- Ghimire, H., McCarrick, R.M., Budil, D.E., Lorigan, G.A., 2009. Significantly improved sensitivity of Q-Band PELDOR/DEER experiments relative to X-Band is observed in measuring the intercoil distance of a leucine zipper motif peptide (GCN4-LZ). *Biochemistry* 48, 5782–5784.
- Ghimire, H., Abu-Baker, S., Sahu, I.D., Zhou, A., Mayo, D.J., Lee, R.T., Lorigan, G.A., 2012a. Probing the helical tilt and dynamic properties of membrane-bound phospholamban in magnetically aligned bicelles using electron paramagnetic resonance spectroscopy. *Biochim. Biophys. Acta* 1818 (3), 645–650.
- Ghimire, H., Hustedt, E.J., Sahu, I.D., Inbaraj, J.J., McCarrick, R., Mayo, D.J., Benedikt, M.R., Lee, R.T., Grosser, S.M., Lorigan, G.A., 2012b. Distance measurements on a dual-labeled TOAC AChR M2(peptide in mechanically aligned DMPC bilayers via dipolar broadening CW-EPR spectroscopy. *J. Phys. Chem. B* 116 (12), 3866–3873.
- Hanson, P., Anderson, D.J., Martinez, G., Millhauser, G., Formaggio, F., Crisma, M.,

Toniolo, C., Vita, C., 1998. Electron spin resonance and structural analysis of water soluble, alanine-rich peptides incorporating TOAC. *Mol. Phys.* 95 (5), 957–966.

Hong, M., Zhang, Y., Hu, F., 2012. Membrane protein structure and dynamics from NMR spectroscopy. *Annu. Rev. Phys. Chem.* 63, 1–24.

Huang, H.W., 2000. Action of antimicrobial peptides: two-state model. *Biochemistry* 39 (29), 8347–8352.

Inbaraj, J.J., Cardon, T.B., Laryukhin, M., Grosser, S.M., Lorigan, G.A., 2006. Determining the topology of integral membrane peptides using EPR spectroscopy. *J. Am. Chem. Soc.* 128, 9549–9554.

Inbaraj, J.J., Laryukhin, M., Lorigan, G.A., 2007. Determining the helical tilt angle of a transmembrane helix in mechanically aligned lipid bilayers using EPR spectroscopy. *J. Am. Chem. Soc.* 129 (25), 7710.

Jackson, M., Mantsch, H.H., Spencer, J.H., 1992. Conformation of magainin-2 and related peptides in aqueous-solution and membrane environments probed by Fourier-Transform Infrared-Spectroscopy. *Biochemistry* 31 (32), 7289–7293.

Judge, P.J., Watts, A., 2011. Recent contributions from solid-state NMR to the understanding of membrane protein structure and function. *Curr. Opin. Chem. Biol.* 15 (5), 690–695.

Karal, M.A., Alam, J.M., Takahashi, T., Levadny, V., Yamazaki, M., 2015. Stretch-activated pore of the antimicrobial peptide, magainin 2. *Langmuir* 31 (11), 3391–3401.

Karim, C.B., Kirby, T.L., Zhang, Z.W., Nesmelov, Y., Thomas, D.D., 2004. Phospholamban structural dynamics in lipid bilayers probed by a spin label rigidly coupled to the peptide backbone. *Proc. Natl. Acad. Sci. U. S. A.* 101 (40), 14437–14442.

Karim, C.B., Zhang, Z.W., Howard, E.C., Torgersen, K.D., Thomas, D.D., 2006. Phosphorylation-dependent conformational switch in spin-labeled phospholamban bound to SERCA. *J. Mol. Biol.* 358 (4), 1032–1040.

Karim, C.B., Zhang, Z., Thomas, D.D., 2007. Synthesis of TOAC spin-labeled proteins and reconstitution in lipid membranes. *Nat. Protoc.* 2, 42–49.

Karp, E.S., Inbaraj, J.J., Laryukhin, M., Lorigan, G.A., 2006. Electron paramagnetic resonance studies of an integral membrane peptide inserted into aligned phospholipid bilayer nanotube arrays. *J. Am. Chem. Soc.* 128 (37), 12070–12071.

Klug, C.S., Feix, J.B., 2008. Methods and applications of site-directed spin labeling EPR spectroscopy. *Methods Cell Biol.* 84, 617–658.

Mangels, C., Kellner, R., Einsiedel, J., Weiglemeier, P.R., Rosch, P., Gmeiner, P., Schwarzeniger, S., 2010. The therapeutically anti-prion active antibody-fragment scF (v)-W226: paramagnetic relaxation-enhanced NMR spectroscopy aided structure elucidation of the paratope-epitope interface. *Journal of Biomolecular Structure. Dynamics* 28 (1), 13–22.

Marassi, F.M., Opella, S.J., 2000. A solid-state NMR index of helical membrane protein structure and topology. *J. Magn. Reson.* 144 (1), 150–155.

Marassi, F.M., Ma, C., Gesell, J.J., Opella, S.J., 2000. Three-dimensional solid-state NMR spectroscopy is essential for resolution of resonances from In-Plane residues in uniformly 15N-Labeled helical membrane proteins in oriented lipid bilayers. *J. Magn. Reson.* 144 (1), 156–161.

Marchetto, R., Schreier, S., Nakae, C.R., 1993. A novel spin-labeled amino acid derivative for use in peptide synthesis: (9-fluorenylmethoxy carbonyl)-2,2,6,6-tetra-methylpiperidine-N-oxyl-4-amino-4-carboxylic acid. *J. Am. Chem. Soc.* 115 (23), 11042–11043.

Marsh, D., Jost, M., Peggion, C., Toniolo, C., 2007. TOAC spin labels in the backbone of alamethicin: EPR studies in lipid membranes. (vol 92, pg 473, 2007). *Biophys. J.* 93 (2), 705.

Marsh, D., 2010. Spin-Label EPR for determining polarity and proticity in biomolecular assemblies transmembrane profiles. *Appl. Magn. Reson.* 37 (1–4), 435–454.

Matsuzaki, K., Murase, O., Tokuda, H., Funakoshi, S., Fujii, N., Miyajima, K., 1994. Orientational and aggregational states of magainin-2 in phospholipid-bilayers. *Biochemistry* 33 (11), 3342–3349.

Matsuzaki, K., Murase, O., Fujii, N., Miyajima, K., 1996. An antimicrobial peptide, magainin 2, induced rapid flip-flop of phospholipids coupled with pore formation and peptide translocation. *Biochemistry* 35 (35), 11361–11368.

Matsuzaki, K., Sugishita, M., Harada, K.-I., Fujii, N., Miyajima, K., 1997. Interactions of an antimicrobial peptide, magainin 2, with outer and inner membranes of Gram-negative bacteria. *Biochimica et Biophysica Acta (BBA). Biomembranes* 1327 (1), 119–130.

Matsuzaki, K., Sugishita, K., Ishibe, N., Ueha, M., Nakata, S., Miyajima, K., Epan, R.M., 1998a. Relationship of membrane curvature to the formation of pores by magainin 2. *Biochemistry* 37 (34), 11856–11863.

Matsuzaki, K., Mitani, Y., Akada K.-y. Murase, O., Yoneyama, S., Zasloff, M., Miyajima, K., 1998b. Mechanism of synergy between antimicrobial peptides magainin 2 and PGaL. *Biochemistry* 37 (43), 15144–15153.

Mayo, D.J., Inbaraj, J.J., Subbaraman, N., Grosser, S.M., Chan, C.A., Lorigan, G.A., 2008. Comparing the structural topology of integral and peripheral membrane proteins utilizing electron paramagnetic resonance spectroscopy. *J. Am. Chem. Soc.* 130 (30), 9656–9657.

Michalek, M., Salnikov, E.S., Bechinger, B., 2013. Structure and topology of the huntingtin 1–17 membrane anchor by a combined solution and solid-state NMR approach. *Biophys. J.* 105 (3), 699–710.

Moraes, L.G.M., Fazio, M.A., Vieira, R.F.F., Nakae, C.R., Miranda, M.T.M., Schreier, S., Daffre, S., Miranda, A., 2007. Conformational and functional studies of gomesin analogues by CD, EPR and fluorescence spectroscopies. *Biochim. Et Biophys. Acta-Biomembr.* 1768 (1), 52–58.

Nakae, C.R., Schreier, S., Paiva, A.C.M., 1983. Synthesis and properties of spin-labeled angiotensin derivatives. *Biochimica et Biophysica Acta (BBA). Protein Struct. Mol. Enzymol.* 742 (1), 63–71.

Nevzorov, A.A., 2011. Orientational and motional narrowing of solid-state NMR lineshapes of uniaxially aligned membrane proteins. *J. Phys. Chem. B* 115 (51), 15406–15414.

Nguyen, L.T., Haney, E.F., Vogel, H.J., 2011. The expanding scope of antimicrobial peptide structures and their modes of action. *Trends Biotechnol.* 29 (9), 464–472.

Opella, S.J., Marassi, F.M., 2004. Structure determination of membrane proteins by NMR spectroscopy. *Chem. Rev.* 104 (8), 3587–3606.

Oren, Z., Shai, Y., 1998. Mode of action of linear amphipathic alpha-helical antimicrobial peptides. *Biopolymers* 47 (6), 451–463.

Park, S.H., Son, W.S., Mukhopadhyay, R., Valafar, H., Opella, S.J., 2009. Phage-induced alignment of membrane proteins enables the measurement and structural analysis of residual dipolar couplings with dipolar waves and lambda-maps. *J. Am. Chem. Soc.* 131 (40), 14140–14141.

Plato, M., Steinhoff, H.-J., Wegener, C., Töring, J.T., Savitsky, A., Möbius, K., 2002. Molecular orbital study of polarity and hydrogen bonding effects on the g and hyperfine tensors of site directed NO spin labelled bacteriorhodopsin. *Mol. Phys.* 100, 3711–3721.

Prongidi-Fix, L., Bertani, P., Bechinger, B., 2007. The membrane alignment of helical peptides from non-oriented N-15 chemical shift solid-state NMR spectroscopy. *J. Am. Chem. Soc.* 129 (27), 8430.

Sahu, I.D., McCarrick, R.M., Lorigan, G.A., 2013. Use of electron paramagnetic resonance to solve biochemical problems. *Biochemistry* 52, 5967–5984.

Sahu, I.D., Hustedt, E.J., Ghimire, H., Inbaraj, J.J., McCarrick, R.M., Lorigan, G.A., 2014a. CW dipolar broadening EPR spectroscopy and mechanically aligned bilayers used to measure distance and relative orientation between two TOAC spin labels on an antimicrobial peptide. *J. Magn. Reson.* 249, 72–79.

Sahu, I.D., Kroncke, B.M., Zhang, R., Dunagan, M.M., Smith, H.J., Craig, A., McCarrick, R.M., Sanders, C.R., Lorigan, G.A., 2014b. Structural investigation of the transmembrane domain of KCNE1 in proteoliposomes. *Biochemistry* 53, 6392–6401.

Sahu, I.D., Mayo, D.J., Subbaraman, N., Inbaraj, J.J., McCarrick, R.M., Lorigan, G.A., 2017. Probing topology and dynamics of the second transmembrane domain (M28) of the acetyl choline receptor using magnetically aligned lipid bilayers (bicelles) and EPR spectroscopy. *Chem. Phys. Lipids* 206, 9–15.

Sato, H., Felix, J.B., 2006. Peptide-membrane interactions and mechanisms of membrane destruction by amphipathic alpha-helical antimicrobial peptides. *Biochim. Et Biophys. Acta-Biomembr.* 1758 (9), 1245–1256.

Schneider, D.J., Freed, J.H., 1989. Calculating slow motional magnetic resonance spectra: a user's guide. In: Berlinger, L.J. (Ed.), *Biological Magnetic Resonance*. Plenum Publishing, New York.

Schreier, S., Bozelli Jr., J.C., Marín, N., Vieira, R.F.F., Nakae, C.R., 2012. The spin label amino acid TOAC and its uses in studies of peptides: chemical, physicochemical, spectroscopic, and conformational aspects. *Biophys. Rev.* 4, 45–66.

Steinhoff, H., Savitsky, A., Wegener, C., Pfeiffer, M., Plato, M., Möbius, K., 2000. High-field EPR studies of the structure and conformational changes of site-directed spin labeled bacteriorhodopsin. *Biochimica et Biophysica Acta (BBA). Bioenergetics* 1457 (3), 253–262.

Strandberg, E., Tremouilhac, P., Wadhwan, P., Ulrich, A.S., 2009. Synergistic transmembrane insertion of the heterodimeric PGaL/magainin 2 complex studied by solid-state NMR. *Biochimica et Biophysica Acta (BBA). Biomembranes* 1788 (8), 1667–1679.

Strandberg, E., Horn, D., Reisser, S., Zerweck, J., Wadhwan, P., Ulrich, A.S., 2016. H-2-NMR and MD simulations reveal membrane-bound conformation of magainin 2 and its synergy with PGaL. *Biophys. J.* 111 (10), 2149–2161.

Tamba, Y., Yamazaki, M., 2005. Single giant unilamellar vesicle method reveals effect of antimicrobial peptide magainin 2 on membrane permeability. *Biochemistry* 44 (48), 15823–15833.

Tamba, Y., Yamazaki, M., 2009. Magainin 2-induced pore formation in the lipid membranes depends on its concentration in the membrane interface. *J. Phys. Chem. B* 113 (14), 4846–4852.

Ulmschneider, M.B., Sansom, M.S.P., Di Nola, A., 2006. Evaluating tilt angles of membrane-associated helices: comparison of computational and NMR techniques. *Biophys. J.* 90 (5), 1650–1660.

Verardi, R., Traaseth, N.J., Shi, L., Porcelli, F., Monfregola, L., De Luca, S., Amodeo, P., Veglia, G., Scaloni, A., 2011. Probing membrane topology of the antimicrobial peptide distinctness by solid-state NMR spectroscopy in zwitterionic and charged lipid bilayers. *Biochimica et Biophysica Acta (BBA). Biomembranes* 1808 (1), 34–40.

Vicente, E.F., Sahu, I.D., Costa-Filho, A.J., Cilli, E.M., Lorigan, G.A., 2015. Conformational changes of the HsDHODH N-terminal microdomain via DEER spectroscopy. *J. Phys. Chem. B* 119 (28), 8693–8697.

Vicente, E.F., Sahu, I.D., Crusca, E., Bassi, L.G.M., Munte, C.E., Costa, A.J., Lorigan, G.A., Cilli, E.M., 2017. HsDHODH microdomain-membrane interactions influenced by the lipid composition. *J. Phys. Chem. B* 121 (49), 11085–11095.

Wright, K., Wakselman, M., Mazaleyrat, J.P., Franco, L., Toffoletti, A., Formaggio, F., Toniolo, C., 2010. Synthesis and conformational characterisation of hexameric beta-peptide foldamers by using double POAC spin labelling and cw-EPR. *Chemistry* 16 (36), 11160–11166.

Yamaguchi, S., Huster, D., Waring, A., Lehrer, R.I., Kearney, W., Tack, B.F., Hong, M., 2001. Orientation and dynamics of an antimicrobial peptide in the lipid bilayer by solid-state NMR spectroscopy. *Biophys. J.* 81 (4), 2203–2214.

Yang, L., Weiss, T.M., Lehrer, R.I., Huang, H.W., 2001. Crystallization of antimicrobial pores in membranes: magainin and protegrin (vol 79, pg 2002, 2000). *Biophys. J.* 80 (2), 1029.

Zasloff, M., Magainins, 1987. A class of antimicrobial peptides from *Xenopus* skin: isolation, characterization of two active forms, and partial cDNA sequence of a precursor. *Proc. Natl. Acad. Sci. U. S. A.* 84 (15), 5449–5453.